Input Shaper Optimization with a Constraint on the Spectrum Distribution ⋆

Vyacheslav Kungurtsev * **Dan Pilbauer**[*, **] **Tomáš Vyhlídal** *
Martin Hromčík * **Wim Michiels** **

* *Czech Technical University in Prague (e-mail: vyacheslav.kungurtsev@fel.cvut.cz, tomas.vyhlidal@fs.cvut.cz, martin.hromcik@fel.cvut.cz)*
** *KU Leuven, Belgium (e-mail: wim.michiels@cs.kuleuven.be, dan.pilbauer@cs.kuleuven.be)*

Abstract: This paper presents a procedure to parametrize input shapers with piecewise equally distributed time delays. The procedure seeks to minimize residual vibrations around an undesirable frequency, but at the same time avoids introducing zeros in the right half plane. This ensures that the introduction of the inverse of the input shaper in a closed feedback loop does not introduce unstable poles in the system. The requirement of stable spectra for the input shaper appears as an additional constraint in a constrained optimization problem that includes minimizing the response time and residual vibrations while preserving required properties of the shaper. The novel introduction of a spectral constraint makes the optimization problem nonsmooth and nonconvex, necessitating special optimization algorithms for its reliable solution. The framework is outlined in detail and the results of the optimization are presented indicating the success of the procedure.

Keywords: time-delay, input shapers, vibration suppression, multi-objective optimisation, Pareto front, spectral abscissa, nonsmooth nonconvex optimization

1. INTRODUCTION

Input shaping was introduced by Smith (1957) in order to remove undesireable oscillatory modes in a system. It has been shown to be effective in performing this task, and has experienced considerable development, Singhose (2009), particularly in order to make the procedure more robust with respect to the exact value of the frequency to be compensated. These include the zero-vibration-derivative (ZVD) and extra-insensitive (EI) shapers, Singer and Seering (1990); Singhose et al. (1994). A comprehensive comparison of various signal shaping techniques is presented in Singer and Seering (1990); Vaughan et al. (2008), and applications are given e.g. in Kim and Singhose (2010); Park et al. (2006).

In Vyhlídal et al. (2013b) an equally distributed delay directly implemented in the shaper was introduced. This was extended to formulating a least-squares optimization approach for directly designing a shaper limiting residual vibrations in Vyhlídal and Hromčík (2015), and subsequently to also optimize the total action time of the shaper design in a multi-criteria bi-objective optimization framework, Pilbauer et al. (2015, 2016)

⋆ Supported by the Czech Science Foundation under project No. 16-17398S. This work has been also supported by the Programme of Interuniversity Attraction Poles of the Belgian Federal Science Policy Office (IAP P6-DYSCO), by OPTEC, the Optimization in Engineering Center of the KU Leuven, and by the project UCoCoS, funded by the European Unions Horizon 2020 research and innovation programme under the Marie Skodowska-Curie Grant Agreement No 675080.

However, input shapers only filter undesirable frequencies of reference signals whereas changes in the disturbance inputs can still excite the oscillations. Recent feedback architecture, proposed in Vyhlídal et al. (2016), suggests to incorporate inverse shaper in the feedback loop. It can be shown that all input channels together with disturbances can be designed to mute undesirable oscillations in a system. On the other hand, chains of infinitely many high frequency zeros of the input shaper turn into poles of the closed loop and affect its dynamics. Input shapers can have a retarded spectrum, Vyhlídal et al. (2016), and if the spectrum of the input shapers has unstable modes it may result in instability in the closed loop system incorporating the inverse shaper. In this paper, we extend the work of Vyhlídal and Hromčík (2015); Pilbauer et al. (2016) by including a negative spectral abscissa as a constraint in the optimization problem defining the input shaper with a distributed delay. The introduction of this constraint is the first use of optimization in stabilizing the spectrum of an input shaper.

The spectral abscissa of a linear system is in general a nonsmooth and nonconvex function of system and controller parameters, and several specialized algorithms developed to minimize such functions, motivated by applications in linear algebra, have appeared. Specifically, a popular algorithm with convergence guarantees is gradient sampling, Burke et al. (2005), while some algorithms without guarantees perform excellently in practice, namely BFGS, Lewis and Overton (2013). These procedures have been shown to be successful in the optimiza-

tion of parametrized matrices appearing in linear systems, Lewis (2007) and has been extended for time delay systems in Vanbiervliet et al. (2008); Kungurtsev et al. (2017). In this paper, we make use of the algorithm SQP-GS Curtis and Overton (2012), which incorporates gradient sampling in a sequential quadratic programming method for extending this previous work to problems with nonsmooth and nonconvex constraints. SQP-GS has shown considerable promise in solving problems with such constraints, but has hitherto never been applied to the design of stable of closed loop systems subject to residual vibrations. This paper is the first known attempt to use these optimization techniques in order to improve the spectrum of an input shaper.

2. BACKGROUND

Following Vyhlídal and Hromčík (2015), we consider an input shaper in the form

$$S(s) = A + \frac{\sum_{k=0}^{N} a_k \mathrm{e}^{-s\tau_k}}{s} \tag{1}$$

with the delays $\tau_k, k = 0...N$ distributed equally on the interval $[0, T]$, where $N > 0$ is the number of coefficients.

Given an oscillatory mode $\hat{s}_z = -\omega\zeta - j\omega\sqrt{1-\zeta^2}$ to be compensated by the shaper, we would like to minimize the residual vibrations in a region $[\omega_{\min}, \omega_{\max}]$, $[\zeta_{\min}, \zeta_{\max}]$ which we discretize in a set of N_ω, N_ζ Chebyshev points, Stewart (1998).

Defining the vector $\mathbf{x} = \begin{bmatrix} A\, a_0\, a_1 \dots a_{N_p} \end{bmatrix}^T$ of gains, the weighted averaged residual vibration in the region is given by, $\mathbf{x}^\intercal H(T)\mathbf{x}$, where,

$$H(T) = \frac{1}{N_\omega N_\zeta} \sum_{k=0}^{N_\omega} \sum_{l=0}^{N_\zeta} e^{2\zeta_l \omega_k T} \Re\left\{ L(\zeta_l, \omega_k, T) L(\zeta_l, \omega_k, T)^T \right\},$$
$$L(\zeta_l, \omega_k, T) = \begin{bmatrix} 1\, g_0\, g_1 \dots g_{N_p} \end{bmatrix},$$
$$g_m = \frac{e^{-(\omega_k\zeta_l - j\omega_k\sqrt{1-\zeta_l^2}\tau_m}}{-(\omega_k\zeta_l - j\omega_k\sqrt{1-\zeta_l^2}.}$$

In addition, we can include equality constraints to compensate the oscillatory mode entirely,

$$\Re\left(A + \frac{1}{\hat{s}_n} \sum_{k=0}^{N_p} a_k e^{-\hat{s}_n \tau_k} \right) = 0,$$
$$\Im\left(A + \frac{1}{\hat{s}_n} \sum_{k=0}^{N_p} a_k e^{-\hat{s}_n \tau_k} \right) = 0.$$

Additional equality constraints

$$\sum_{k=0}^{N_p} a_k = 0,\ A - \sum_{k=0}^{N_p} a_k \tau_k = 1,$$

guarantee the static gain of the shaper equal to one. Then the following inequality constraints

$$-\sum_{k=0}^{l} a_k < 1, l = 0, 1, 2..N_p - 1,$$

ensure a non-decreasing step response. For more details see, Vyhlídal and Hromčík (2015), Pilbauer et al. (2016).

The original multi-objective optimization problem, given in Pilbauer et al. (2016), for shaper design takes the form,

$$\min_{T,\mathbf{x}} \left\{ \left(\frac{T}{T_{\text{nom}}} \right)^2,\ \frac{\mathbf{x}^\intercal H(T)\mathbf{x}}{R_{\text{nom}}^2} \right\},$$
$$\text{subject to } \begin{cases} A_1(T)\mathbf{x} \geq b_1, \\ A_2(T)\mathbf{x} = b_2. \end{cases} \tag{2}$$

To simplify the exposition, we shall be interested in the input shaper returned for a given value of the total time T, so we take T as given and solve a simpler optimization task,

$$\min_{\mathbf{x}} \frac{\mathbf{x}^\intercal H(T)\mathbf{x}}{R_{\text{nom}}^2},\ \text{subject to } \begin{cases} A_1(T)\mathbf{x} \geq b_1, \\ A_2(T)\mathbf{x} = b_2. \end{cases} \tag{3}$$

If we ensure that the parameter $A > 0$ by including this as an extra inequality constraint, then the spectrum is retarded, Vyhlídal and Hromčík (2015). In this case, the number of right half plane zeros is finite, Hale and Lunel (2013) and optimization procedures can be used to force the spectral abscissa to be strictly negative. Note that if $A = 0$ the spectrum is neutral with possibly infinitely many right-half plane zeros.

2.1 Introduction Example

It can easily be shown that by solving (3) as a function of T, the Pareto front of the multi-objective optimization problem (2) is obtained. The Pareto front gives the tradeoff in terms of total impulse time and the resulting residual vibrations.

To introduce the problem, we consider the shaper (1) with $N = 18$. Let us note that as $N \to \infty$, the delay distribution approaches the distribution of a classical shaper with lumped delays, which is time optimal, but has a neutral spectrum, Vyhlídal et al. (2013a). As we are interested in the spectral properties of the input shaper, we seek a number that is physically realistic, while large enough to be challenging for spectral optimization, and while small enough to still have a discernible retarded spectrum.

We consider an initial step gain $A = 0.01$ and seek to minimize the oscillations associated with $\omega = 24s^{-1}$ and $\zeta = 0.1$, as described for the pendulum system described in Vyhlídal et al. (2016). The Pareto front arising from (3) is given in Fig. 1. For the demonstration purposes, the input shaper corresponding to a total time of $T = 0.4s$ is considered. In Figure 2 we show the step and impulse responses and the resultant residual vibrations for the input shaper determined at the solution of this optimization problem. The step response satisfies the non-decreasing condition and the time of the response

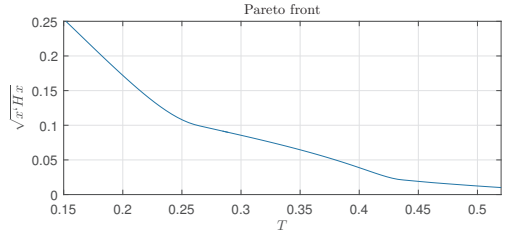

Fig. 1. Pareto front for the solution of (3).

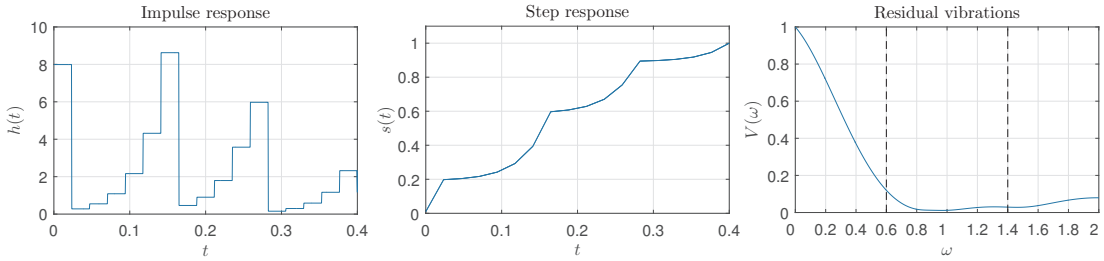

Fig. 2. The properties of the input shaper for the solution of (3) at $T = 0.4s$

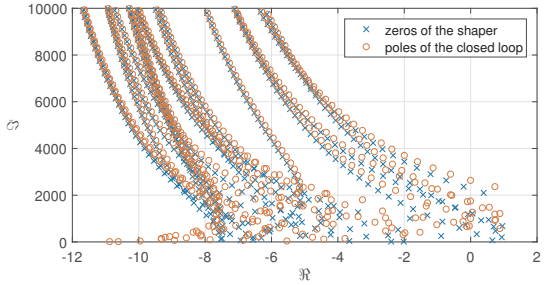

Fig. 3. Spectra of shaper zeros (×) and closed loop poles (○) of system with an inverse shaper - the optimal shaper for $T = 0.4s$ *without* the spectral constraint.

corresponds to the $T = 0.4s$ point selected from the Pareto front in Fig. 1. Impulse response, being the derivative of the step response, shows the corresponding change of slope of the step response. Note that the residual vibration function (with a normalized frequency) is not going to zero for the nominal frequency because the requirement for placing the exact zero is not included in the optimization procedure–this results in a flatter residual vibration function on the given region of parameters.

In order to justify the aim of this paper, we plot the spectrum of zeros in Figure 3, calculated using the algorithm described in Michiels (2011), Wu and Michiels (2012). Notice that the spectrum is retarded, but there are a large number of zeros that are to the right of the imaginary axis, suggesting the shaper is likely to induce the close loop instability if implemented according to Vyhlídal et al. (2016), which will be discussed further on.

2.2 Inverse shaper in the feedback loop

The scheme with an inverse shaper, Vyhlídal et al. (2016) which motivates this work is shown in Figure 4 where $C(s)$ is a controller, the oscillatory system to be compensated is $F(s)$, the shaper is $S(s)$, and there is a system $G(s)$. We denote the reference signal as w, the controller input e, the controller output u, input shaper output v, input/output disturbance d_1/d_2, output x and z, observable y.

Note that the transfer functions from w, d_1, d_2 to y here are

$$T_{wy} = \frac{CG}{1+CG\frac{1}{S}}F = \frac{CGS}{(S+CG)}\frac{F_N}{F_D},$$
$$T_{d_1y} = \frac{G}{1+CG\frac{1}{S}}F = \frac{GS}{(S+CG)}\frac{F_N}{F_D},$$
$$T_{d_2y} = \frac{1}{1+CG\frac{1}{S}}F = \frac{S}{(S+CG)}\frac{F_N}{F_D},$$

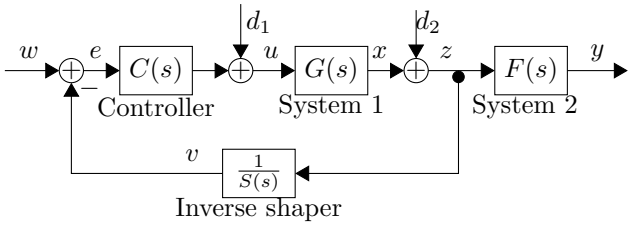

Fig. 4. Control scheme implementing the inverse shaper in a closed loop.

and so if the shaper S has zeros placed as zeros of F_D this result in their cancellation in all the considered transfer functions. However, it also introduces zeros of its own into the roots of the characteristic equation of $S + CG$.

It has been widely discussed in Vyhlídal et al. (2016) that the high frequency poles of the closed loop tend to match the high frequency spectrum of the shaper $S(s)$ zeros. Thus, the high frequency right half plane zeros are risky for the closed loop dynamics. Below, as the main result of the paper, we define and solve an optimization problem which includes the requirement on all the zeros to be located to the left of the imaginary axis.

3. OPTIMIZATION WITH SPECTRAL CONSTRAINT

We can add a spectral constraint to the optimization problem above, to form,

$$\min_{\mathbf{x}} \frac{\mathbf{x}^\intercal H(T)\mathbf{x}}{R_{\text{nom}}^2}, \text{ subject to } \begin{cases} A_1(T)\mathbf{x} \geq b_1, \\ A_2(T)\mathbf{x} = b_2, \\ \alpha(\mathbf{x}, T) \leq \alpha_c, \end{cases} \quad (4)$$

where $\alpha(\mathbf{x}, T)$ is the spectral abscissa, the maximum real part of the eigenvalues of the shaper, not including the zeros placed exactly by constraint in the optimization. The parameter $\alpha_c < 0$ is some threshold value close to zero.

This problem is now non-convex and non-smooth, as the spectral abscissa function is itself non-convex and non-smooth, Burke and Overton (2001). Algorithms for these problems are limited, and typically HANSO, Overton (2009), which uses a combination of a BFGS and gradient sampling procedure, is used to minimize a nonsmooth non-convex function. However, in this case the nonsmooth non-convex function is in the constraint, necessitating the use of appropriate constrained optimization procedures. We use the algorithm SQP-GS given in Curtis and Overton (2012). This is an SQP algorithm that uses an exact l1 merit function to enforce global convergence. The gradient information for the non-smooth functions in the problem, in this case, $\alpha(\mathbf{x}, T)$ is formed by carefully sampling the functions near the current point. The design of stable input

shapers along these lines presents a novel opportunity to test the efficacy and robustness of the SQP-GS algorithm on a challenging problem.

3.1 Global and local optimization

The function $\alpha(\mathbf{x}, T)$ is typically nonsmooth and nonconvex, which suggests that possibility that (4) could have multiple local minima. How pervasive they are can determine the relative importance of global versus local strategies in solving the problem, i.e., if there are a large number of local minima, then a careful random starting point selection procedure (stochastic globalization approach) will impact the performance of a procedure to solve (4) more than the reliability of the local optimization solver, whereas the existence of just a few peaks of local minimizers suggests that any rudimentary sampling procedure may suffice and the performance of the local optimization software is more crucial to efficiently and reliably finding the solution.

We investigated $\alpha(\mathbf{x}, T)$ with respect to two different parameters, taking the others as constant. It was found out that the quantity of local minimizers is expected to be fairly low. Thus we do not concern ourselves with using the best global optimization techniques available.

3.2 Description of the Algorithm

Consider a standard nonlinear program (NLP) with objective function f and constraint functions c^j,

$$\min_x \ f(x) \text{ s.t. } c^j(x) \leq 0 \, j \in \{1, ..., m\}.$$

In our case, the objective $f(x)$ is the residual vibrations, and the constraints c^j include the linear constraints defining a proper distributed delay system and the additional spectral constraint.

SQP-GS solves this problem by repeatedly solving a series of quadratic programs. At each iteration, given the current point x_k, the subproblem,

$$\begin{aligned} \min_{d,z,r} \ & \rho z + \sum_{j=1}^{m} r^j + \frac{1}{2} d^T H_k d \\ \text{s.t. } & f(x_k) + \nabla f(x)^T d \leq z, \, \forall x \in \mathcal{B}^f_{\epsilon,k} \\ & c^j(x_k) + \nabla c^j(x)^T d \leq r^j, \, \forall j \in \{1, ..., m\}, \forall x \in \mathcal{B}^{c^j}_{\epsilon,k} \end{aligned}$$

is solved, which is a subproblem for the NLP with the objective and constraints weighed by the penalty parameter ρ. The sets $\mathcal{B}^f_{\epsilon,k}$ and $\{\mathcal{B}^{c^j}_{\epsilon,k}\}_{j=1}^m$ are sets of points sampled at which ∇f and ∇c are evaluated. Here H_k is a BFGS estimate of the Lagrangian Hessian. In our case, for solving (4), since the only nonsmooth function is the spectral constraint, only this function needs to be sampled for, and the subproblem reduces to,

$$\begin{aligned} \min_{d,z,r} \ & \rho z + r^1 - r_1^2 + r_2^2 + r^3 + \frac{1}{2} d^T H_k d \\ \text{s.t. } & \mathbf{x}_k^\intercal H(T) \mathbf{x}_k + 2(H(T)\mathbf{x}_k)^T d \leq z, \\ & b_1 - A_1(T)(\mathbf{x}_k + d) \leq r^1, \\ & r_2^1 \leq A_2(T)(\mathbf{x}_k + d) - b_2 \leq r_2^2, \\ & \alpha(\mathbf{x}_k, T) - \alpha_c + \nabla_x \alpha(\mathbf{x}_k, T)(x)^T d \leq r^3, \forall x \in \mathcal{B}^\alpha_{\epsilon,k}. \end{aligned}$$

Note that by Rademacher's Theorem, Rockafellar and Wets (2009), the set of non-differentiable points for a nonsmooth function is confined to a set of measure zero for locally Lipschitz functions, and thus the procedure, linked to a linesearch enforcing descent for the appropriate merit function, is provably convergent for Lipschitz functions. The spectral abscissa of a time delay system is, as a function of system parameters, in general not everywhere Lipschitz continuous, but under mild condition it is differentiable almost everywhere, Burke and Overton (2001), suggesting the algorithm is appropriate, which is consistent with the authors' Curtis and Overton (2012) numerical experience and intended applications. We note that Curtis et al. (2015) presents an algorithm for constrained non-convex nonsmooth optimization with numerical results indicating faster performance relative to SQP-GS, and future research and analysis of stable input shapers will use this algorithm, however the code is not yet publicly available.

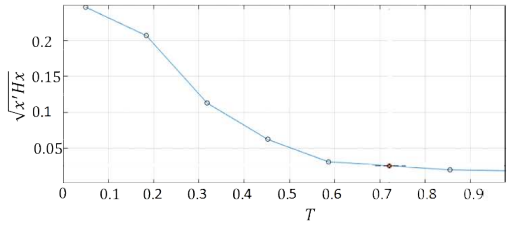

Fig. 5. Pareto front across α for the solution of (4).

4. CASE STUDY EXAMPLE

Consider the specification of the shaper as in the introductory example in Section 2.1, with $A = 0.01$, $\omega = 24s^{-1}$ and $\zeta = 0.1$. Additionally we require that all zeros are located to the left of the imaginary axis. Analogously to Figure 1 we can extract the Pareto front in Figure 5. The Pareto front with the additional constraint remains comparable, however towards the more robust direction it declines less steeply, indicating that satisfying the spectral constraint does make it more difficult to design a fast shaper that minimizes residual vibrations. In general, for any level of residual vibration or total time, the corresponding value of the other one is about double what it was for the case without a stabilized spectrum.

The SQP-GS algorithm is, however, very slow, and construction of the Pareto front for (4) is several orders of magnitude more time consuming than the construction of the Pareto front for (3). However, in the applications of interest, its performance is not important (i.e., it does not need to run in real-time).

We again analyze the shaper solution corresponding to the total response time $T = 0.4s$. As can be seen, the spectrum of zeros is entirely stable, see Figure 8, while retaining its general shape. In this case we have $\alpha_c < 0$ indicating that the constraint is active.

The properties of the new shaper are given in Figure 6. In comparison with previous shaper in Fig. 2, the step and impulse responses are smoother. Resulting residual vibrations are slightly higher in the lower frequency range, but comparable in the higher frequency range.

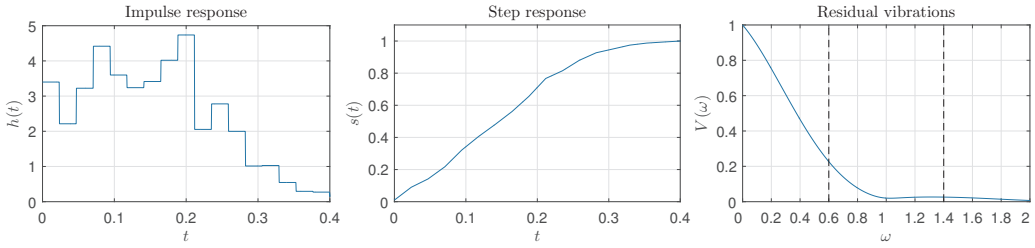

Fig. 6. The properties of the input shaper with stable zeros at $T = 0.4s$.

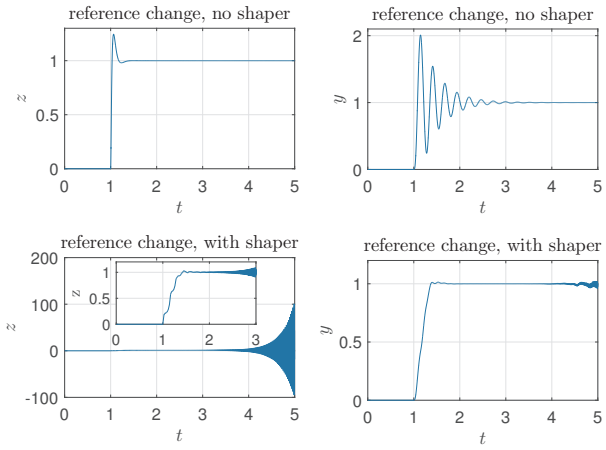

Fig. 7. The reference response of the full system, upper - without a shaper, lower - with unstable shaper.

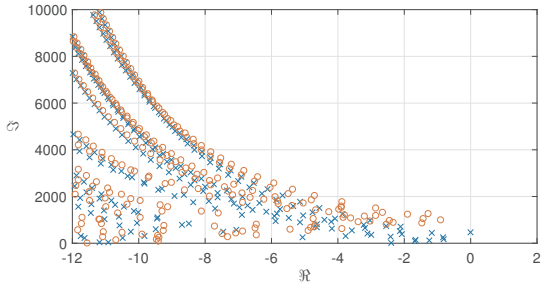

Fig. 8. Spectra of shaper zeros (×) and closed loop poles (○) of system with an inverse shaper - the optimal shaper for $T = 0.4s$ *with* the spectral constraint.

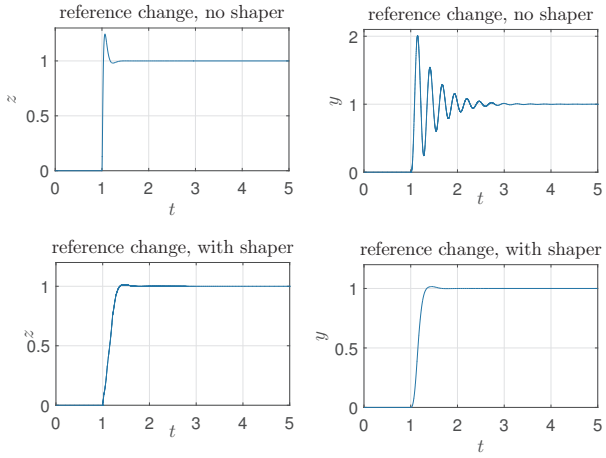

Fig. 9. The reference response of the full system, upper - without a shaper, lower - with stable shaper.

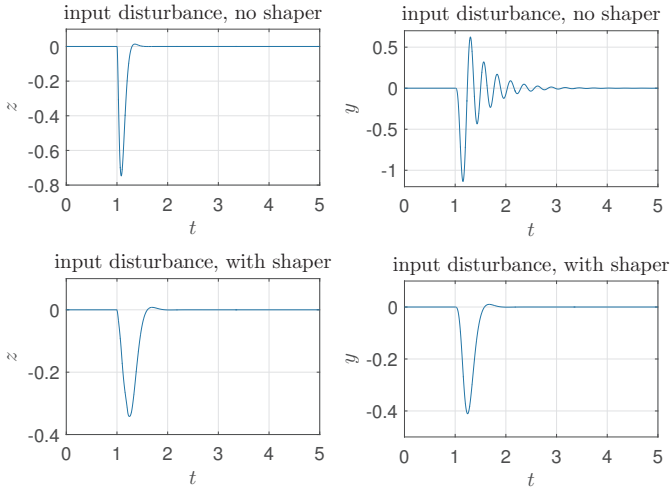

Fig. 10. The full system response to the input disturbance, upper - without a shaper, lower - with stable shaper.

4.1 Closed Loop System Example

For the closed loop system with the shaper applied as its inverse given in scheme in Fig. 4, consider the system $G(s) = \frac{1}{Ms^2+bs}$ with $M = 0.9$ and $b = 7.47$ and PID controller $C(s) = r_0 + \frac{r_d N s}{s+N} + \frac{r_i}{s}$ with $N = 200$, $r_0 = 1060$, and $r_d = 40$, as in Vyhlídal et al. (2013a) which stabilizes the system without inverse shaper. Two cases are considered for the inverse shaper tuned to compensate the oscillatory mode of the flexible part - System 2 - with $F(s) = \frac{\omega^2}{s^2+2\zeta\omega s+\omega^2}$, $\omega = 24s^{-1}$ and $\zeta = 0.1$: i) the shaper with unstable spectrum of zeros designed in Introduction Example, and ii) the shaper with stable spectrum designed in this Case Study Example section.

The spectrum of the closed loop system with the unstable input shaper is given in Figure 3. It can be seen that there is a strong correspondence between the zeros of the input shaper and the poles of the closed loop system with the inverse of the shaper included (note that the matching gets better as the moduli of the roots increase), suggesting that without the spectral constraint in designing the input shaper, the resulting control system would not be exponentially stable. Indeed, the system response can be seen in Figure 7. As expected, the output without the shaper has the undesireable oscillations, and with the shaper, these oscillations are dampened, at the cost of instability at a later time due to high frequency unstable poles.

When we use the input shaper with stabilized spectra, we see that the closed loop system poles are stable, in Figure 8. Furthermore, it can be seen from both the set-

point and disturbance responses in Figures 9 and 10, that the system's oscillations are successfully damped, and yet the system remains stable.

5. CONCLUSION

In this paper we analyzed the design of an input shaper that minimizes the total residual vibrations around an undesirable oscillatory frequency, as done in previous work, while also constraining the spectral abscissa to be sufficiently negative. This is likely to ensure stable performance when the shaper is introduced in a feedback system as its inverse. In order to solve the resulting optimization problem, which is a constrained nonconvex nonsmooth problem, we used an algorithm particularly designed for such problems. We showed that indeed the algorithm was successful at finding an input shaper that minimized the total response time and residual vibrations while keeping the spectral abscissa in the stable left half plane. This presents a novel contribution in the design of input shapers for dampening oscillations, in presenting a framework consistent with the previously developed optimization approach to designing input shapers that stabilizes the poles of the shaper and in turn avoids unstable closed loop behavior upon introduction of the input shaper. In future work we will incorporate this procedure in a real system and showcase the closed loop performance and stability.

REFERENCES

Burke, J.V., Lewis, A.S., and Overton, M.L. (2005). A robust gradient sampling algorithm for nonsmooth, nonconvex optimization. *SIAM J. on Optimization*, 15(3), 751–779.

Burke, J.V. and Overton, M.L. (2001). Variational analysis of non-lipschitz spectral functions. *Mathematical Programming*, 90(2), 317–351.

Curtis, F.E., Mitchell, T., and Overton, M.L. (2015). A bfgs-sqp method for nonsmooth, nonconvex, constrained optimization and its evaluation using relative minimization profiles. Technical report, New York University.

Curtis, F.E. and Overton, M.L. (2012). A sequential quadratic programming algorithm for nonconvex, nonsmooth constrained optimization. *SIAM J. on Optimization*, 22(2), 474–500.

Hale, J.K. and Lunel, S.M.V. (2013). Introduction to functional differential equations. 99.

Kim, D. and Singhose, W. (2010). Performance studies of human operators driving double-pendulum bridge cranes. *Control Engineering Practice*, 18(6), 567–576.

Kungurtsev, V., Michiels, W., and Diehl, M. (2017). An inequality constrained SL/QP method for minimizing the spectral abscissa of time delay systems. *to appear in Advances in Time Delay Systems*.

Lewis, A.S. (2007). Nonsmooth optimization and robust control. *Annual Reviews in Control*, 31(2), 167–177.

Lewis, A.S. and Overton, M.L. (2013). Nonsmooth optimization via quasi-newton methods. *Mathematical Programming*, 141(1-2), 135–163.

Michiels, W. (2011). Spectrum-based stability analysis and stabilisation of systems described by delay differential algebraic equations. *IET control theory & applications*, 5(16), 1829–1842.

Overton, M. (2009). Hanso: a hybrid algorithm for nonsmooth optimization. *Available from cs. nyu. edu/overton/software/hanso*.

Park, J., Chang, P.H., Park, H.S., and Lee, E. (2006). Design of learning input shaping technique for residual vibration suppression in an industrial robot. *IEEE/ASME Trans. on Mechatronics*, 11(1), 55–65.

Pilbauer, D., Michiels, W., and Vyhlídal, T. (2015). Distributed delay input shaper design by optimizing smooth kernel functions. *TW reports, TW663, 25pp. Leuven, Belgium: Department of Computer Science, KU Leuven*.

Pilbauer, D., Michiels, W., and Vyhlídal, T. (2016). Multicriteria optimisation design of shapers with piece-wise equally distributed time-delay. In *Proc. of the 13th IFAC Workshop on Time-Delay Systems*.

Rockafellar, R.T. and Wets, R.J.B. (2009). *Variational analysis*, volume 317. Springer Science & Business Media.

Singer, N.C. and Seering, W.P. (1990). Preshaping command inputs to reduce system vibration. *J. of Dynamic Systems, Measurement, and Control*, 112(1), 76–82.

Singhose, W. (2009). Command shaping for flexible systems: A review of the first 50 years. *Int. J. of Precision Engineering and Manufacturing*, 10(4), 153–168.

Singhose, W., Seering, W., and Singer, N. (1994). Residual vibration reduction using vector diagrams to generate shaped inputs. *J. of Mechanical Design*, 116(2), 654–659.

Smith, O.J. (1957). Posicast control of damped oscillatory systems. *Proc. of the IRE*, 45(9), 1249–1255.

Stewart, G.W. (1998). *Afternotes goes to graduate school: lectures on advanced numerical analysis*. Siam.

Vanbiervliet, J., Verheyden, K., Michiels, W., and Vandewalle, S. (2008). A nonsmooth optimisation approach for the stabilisation of time-delay systems. *ESAIM: Control, Optimisation and Calculus of Variations*, 14(3), 478–493.

Vaughan, J., Yano, A., and Singhose, W. (2008). Comparison of robust input shapers. *J. of Sound and Vibration*, 315(4), 797–815.

Vyhlídal, T., Hromčík, M., Kučera, V., and Anderle, M. (2016). On feedback architectures with zero-vibration signal shapers. *IEEE Trans. on Automatic Control*, 61(8), 2049–2064.

Vyhlídal, T. and Hromčík, M. (2015). Parameterization of input shapers with delays of various distribution. *Automatica*, 59, 256–263.

Vyhlídal, T., Hromčík, M., and Kučera, V. (2013a). Inverse signal shapers in effective feedback architecture. In *Proc. European Control Conference*, 4418–4423.

Vyhlídal, T., Kučera, V., and Hromčík, M. (2013b). Signal shaper with a distributed delay: Spectral analysis and design. *Automatica*, 49(11), 3484–3489.

Wu, Z. and Michiels, W. (2012). Reliably computing all characteristic roots of delay differential equations in a given right half plane using a spectral method. *J. of Computational and Applied Mathematics*, 236(9), 2499–2514.